1521-0111/12/8106-800–810$25.00
MOLECULAR PHARMACOLOGY
Vol. 81, No. 6
77206/3770094

Mol Pharmacol 81:800–810, 2012

Differential Expression and Function of Alternative Splicing Variants of Human Liver X Receptor α

Kaori Endo-Umeda, Shigeyuki Uno, Ko Fujimori, Yoshikazu Naito, Koichi Saito, Kenji Yamagishi,[1] Yangsik Jeong, Hiroyuki Miyachi, Hiroaki Tokiwa, Sachiko Yamada, and Makoto Makishima

Division of Biochemistry, Department of Biomedical Sciences, Nihon University School of Medicine, Tokyo, Japan (K.E.-U., S.U., S.Y., M.M.); Laboratory of Biodefense and Regulation, Osaka University of Pharmaceutical Sciences, Osaka, Japan (K.F.); Environmental Health Science Laboratory, Sumitomo Chemical Co., Ltd., Osaka, Japan (Y.N., K.S.); Research Information Center for Extremophile (K.Y.) and Department of Chemistry (H.T.), Faculty of Science, Rikkyo University, Tokyo, Japan; Department of Biochemistry, Institute of Lifestyle Medicine, and Nuclear Receptor Research Consortium, Yonsei University Wonju College of Medicine, Gangwon-do, Republic of Korea (Y.J.); and Graduate School of Medicine, Dentistry, and Pharmaceutical Sciences, Okayama University, Okayama, Japan (H.M.)

Received December 14, 2011; accepted March 7, 2012

ABSTRACT

The liver X receptor α (LXRα) is a nuclear receptor that is involved in regulation of lipid metabolism, cellular proliferation and apoptosis, and immunity. In this report, we characterize three human LXRα isoforms with variation in the ligand-binding domain (LBD). While examining the expression of LXRα3, which lacks 60 amino acids within the LBD, we identified two novel transcripts that encode LXRα-LBD variants (LXRα4 and LXRα5). LXRα4 has an insertion of 64 amino acids in helix 4/5, and LXRα5 lacks the C-terminal helices 7 to 12 due to a termination codon in an additional exon that encodes an intron in the LXRα1 mRNA. LXRα3, LXRα4, and LXRα5 were expressed at lower levels compared with LXRα1 in many human tissues and cell lines. We also observed weak expression of LXRα3 and LXRα4 in several tissues of mice. LXR ligand treatment induced differential regulation of LXRα isoform mRNA expression in a cell type-dependent manner. Whereas LXRα3 had no effect, LXRα4 has weak transactivation, retinoid X receptor (RXR) heterodimerization, and coactivator recruitment activities. LXRα5 interacted with a corepressor in a ligand-independent manner and inhibited LXRα1 transactivation and target gene expression when overexpressed. Combination of LXRα5 cotransfection and LXRα antagonist treatment produced additive effects on the inhibition of ligand-dependent LXRα1 activation. We constructed structural models of the LXRα4-LBD and its complexes with ligand, RXR-LBD, and coactivator peptide. The models showed that the insertion in the LBD can be predicted to disrupt RXR heterodimerization. Regulation of LXRα pre-mRNA splicing may be involved in the pathogenesis of LXRα-related diseases.

Introduction

Liver X receptor α (LXRα; NR1H3) and LXRβ (NR1H2) are transcription factors of the nuclear receptor superfamily (Tontonoz and Mangelsdorf, 2003; Makishima, 2005). Whereas LXRβ is ubiquitously expressed, LXRα is localized to the liver, adipose tissue, small intestine, and macrophages. Both receptors are activated by oxysterols and have been linked to pathways involved in fatty acid and cholesterol homeostasis. LXRs bind preferentially to LXR-responsive elements (LXREs) that consist of a two-hexanucleotide (AGGTCA or a related sequence) direct repeat motif separated by four nucleotides (direct repeat 4) as a heterodimer with retinoid X receptor (RXR; NR2B). LXRs regulate intestinal absorption and biliary excretion of cholesterol by inducing the expression of target genes

This work was supported in part by the Ministry of Education, Culture, Sports, Science, and Technology of Japan [Grant-in-Aid for Scientific Research on Priority Areas 18077005] (to M.M.).

[1] Current affiliation: Department of Chemical Biology and Applied Chemistry, College of Engineering, Nihon University, Fukushima, Japan.

Article, publication date, and citation information can be found at http://molpharm.aspetjournals.org.
http://dx.doi.org/10.1124/mol.111.077206.

ABBREVIATIONS: LXR, liver X receptor; LXRE, LXR-responsive element; RXR, retinoid X receptor; ABC, ATP-binding cassette; CYP7A, cholesterol 7α-hydroxylase; SREBP, sterol regulatory element-binding protein; LBD, ligand-binding domain; T0901317, *N*-(2,2,2-trifluoro-ethyl)-*N*-[4–(2,2,2-trifluoro-1-hydroxy-1-trifluoromethyl-ethyl)-phenyl]-benzenesulfonamide; GW3965, 3-[3-[*N*-(2-chloro-3-trifluoromethylbenzyl)-(2,2-diphenylethyl)amino]propyloxy]phenylacetic acid hydrochloride; HEK, human embryonic kidney; FBS, fetal bovine serum; PCR, polymerase chain reaction; siRNA, small interfering RNA; CMV, cytomegalovirus; EMSA, electrophoretic mobility shift assay; DBD, DNA-binding domain; AF2, activation function 2; SMRT, silencing mediator of retinoic acid and thyroid hormone receptor; N-CoR, nuclear receptor corepressor; SRC, steroid receptor coactivator; DRIP205, vitamin D receptor-interacting protein 205; PPAR, peroxisome proliferator-activated receptor.

such as the ATP-binding cassette (ABC) transporters ABCA1, ABCG5, and ABCG8 (Repa and Mangelsdorf, 2002; Tontonoz and Mangelsdorf, 2003). LXRα stimulates the conversion of cholesterol to bile acids by cholesterol 7α-hydroxylase (CYP7A) in rodents. LXRs stimulate reverse cholesterol transport from peripheral tissues and exhibit antiatherogenic activity. LXR activation also stimulates lipogenesis in the liver by inducing lipogenic genes, including sterol regulatory element-binding protein-1c (SREBP-1c), fatty acid synthase, and stearoyl-coenzyme A desaturase-1 (Schultz et al., 2000). Studies using LXR-null mice and synthetic LXR ligands have also demonstrated that LXRs are involved in the regulation of cellular proliferation and apoptosis (Blaschke et al., 2004; Joseph et al., 2004; Valledor et al., 2004; Uno et al., 2009).

Three human LXRα isoforms (α1, α2, and α3) have been identified that are derived from a single gene as a result of alternate promoter usage and alternative splicing of pre-mRNA (Chen et al., 2005). LXRα1 is the originally identified isoform (Willy et al., 1995), LXRα2 lacks the N-terminal 45 amino acids of LXRα1, and LXRα3 lacks 50 amino acids in the ligand-binding domain (LBD) (Chen et al., 2005). Like different isoforms of other nuclear receptors, LXRα isoforms have distinct expression patterns and altered transcriptional activity, suggesting that the expression of the isoforms modulates LXR signaling. In this study, we isolated and identified two novel LXRα isoforms, LXRα4 and LXRα5, and investigated the roles of LXRα isoforms with functional assays and molecular modeling studies.

Materials and Methods

Chemical Compounds. T0901317 (*N*-(2,2,2-trifluoro-ethyl)-*N*-[4–(2,2,2-trifluoro-1-hydroxy-1-trifluoromethyl-ethyl)-phenyl]-benzenesulfonamide) was purchased from Cayman Chemical Company (Ann Arbor, MI), 24(*S*),25-epoxycholesterol was from Enzo Life Science (Farmingdale, NY), 22(*R*)-hydroxycholesterol and 22(*S*)-hydroxycholesterol were from Steraroids (Newport, RI), and arachidonic acid and linolenic acid were from Sigma-Aldrich (St. Louis, MO). GW3965 (3-[3-[*N*-(2-chloro-3-trifluoromethylbenzyl)-(2,2-diphenylethyl)amino]propyloxy]phenylacetic acid hydrochloride) was synthesized as reported previously (Noguchi-Yachide et al., 2007).

Cell Culture. Human embryonic kidney (HEK) 293 cells (RIKEN Cell Bank, Tsukuba, Japan) were cultured in Dulbecco's modified Eagle's medium containing 5% fetal bovine serum (FBS), 100 unit/ml penicillin, and 100 μg/ml streptomycin at 37°C in a humidified atmosphere containing 5% CO_2. Human hepatocellular carcinoma HepG2 (RIKEN Cell Bank), colon carcinoma HCT116, SW480, teratocarcinoma NT2/D1 (American Type Culture Collection, Manassas, VA), and immortalized keratinocyte HaCaT cells (kindly provided by Dr. Tadashi Terui, Department of Dermatology, Nihon University School of Medicine) were cultured in Dulbecco's modified Eagle's medium containing 10% FBS. Human colon carcinoma Caco-2, osteosarcoma MG63, neuroblastoma SK-N-SH cells (RIKEN Cell Bank) were maintained in minimal essential medium containing 10% FBS, and myeloid leukemia U937, HL60, THP-1 (RIKEN Cell Bank), and breast carcinoma MCF-7 cells (American Type Culture Collection) were maintained in RPMI 1640 medium containing 10% FBS.

Animals. C57BL/6J mice were obtained from Charles River Laboratories Japan (Yokohama, Japan) and Lxrα(−/−)/Lxrβ(−/−) mice were provided by Dr. Mangelsdorf (University of Texas Southwestern Medical Center at Dallas, TX) (Repa et al., 2000). Mice were maintained under controlled temperature (23 ± 1°C) and humidity (45–65%) with free access to water and chow (Laboratory Animal Diet MF; Oriental Yeast, Tokyo, Japan). Tissue samples were collected from male mice between 8 and 9 weeks of age. The experimental protocol adhered to the Guidelines for Animal Experiments of the Nihon University School of Medicine and was approved by the Ethics Review Committee for Animal Experimentation of Nihon University School of Medicine.

Reverse Transcription and Real-Time Quantitative Polymerase Chain Reaction. Total RNAs from samples were prepared by the acid guanidine thiocyanate-phenol/chloroform method (Ishizawa et al., 2008). cDNAs were synthesized using the ImProm-II Reverse Transcription system (Promega Corporation, Madison, WI). cDNA panels of several human tissues were purchased from Takara Bio Inc. (Otsu, Japan). Real-time polymerase chain reaction (PCR) was performed on the ABI PRISM 7000 Sequence Detection System (Applied Biosystems, Foster City, CA) using Power SYBR Green PCR Master Mix (Applied Biosystems). Primer sequences are listed in Tables 1 and 2. The mRNA values were normalized to the expression level of glyceraldehyde-3-phosphate dehydrogenase mRNA.

RNA Interference. Small interfering RNAs (siRNAs) directed against LXRα (siLXRα-1; Dharmacon RNA Technologies, Lafayette, CO), and control siRNA were purchased from Thermo Fisher Scientific (Waltham, MA). siRNAs against LXRα (siLXRα-2; 5′-AGA AAC UGA AGC GGC AAG A-3′) and LXRα/β (siLXRα/β; 5′-CAU CAA CCC CAU CUU CGA G-3′) were designed by the laboratory of author Y.J. siRNA oligonucleotides were transfected into HaCaT cells and HepG2 cells using DharmaFECT1 reagent (Thermo Fisher Scientific) and Trans IT-TKO Reagent (Mirus Bio, Madison, WI), respectively, according to the manufacturer's instructions.

TABLE 1
Primer sequences for real-time quantitative reverse transcription-PCR (human)

Gene	Sequence (5′→3′)	Amplicon Size
		bp
LXRα1		
Forward	CTG CGA TCG AGG TGA TGC TT	197
Backward	ACT ACG GCT CAA ACG GAA C	
LXRα3		
Forward	TGA AGC GGC AAG AGG AGG AA	166
Backward	AGC TCA GTG CCA CTA CGA AG	
LXRα4		
Forward	CGT TTG AGG TTT GCT GCT TG	233
Backward	ACT ACG GCT CAA ACG GAA C	
LXRα5		
Forward	CTG CGA TCG AGG TGA TGC TT	155
Backward	GTT AGT ACC GAG TTA CGT CG	
GAPDH		
Forward	ACT TCG CTC AGA CAC CAT GG	139
Backward	GGG AAG TAA CTG GAG TTG ATG	

GAPDH, glyceraldehyde-3-phosphate dehydrogenase.

TABLE 2
Primer sequences for real-time quantitative reverse transcription-PCR (mouse)

Gene	Sequence (5′→3′)	Amplicon Size
		bp
LXRα1		
Forward	CTG CAA TCG AGG TCA TGC TT	198
Backward	GCA GAG CAA ACT CAG CAT CA	
LXRα3		
Forward	TGA AGC GGC AAG AAG AGG AA	189
Backward	CTC TCC AGA AGC ATG ACC GT	
LXRα4		
Forward	CCT GTC TGA AAG ATG CTG CT	216
Backward	GCA GAG CAA ACT CAG CAT CA	
GAPDH		
Forward	TGC ACC ACC AAC TGC TTA G	176
Backward	GAT GCA GGG ATG ATG TTC	

GAPDH, glyceraldehyde-3-phosphate dehydrogenase.

Western Blotting Analysis. For endogenous LXR proteins, nuclear extracts were prepared as described previously (Inaba et al., 2007). The proteins were separated by SDS-polyacrylamide gel electrophoresis and were transferred to a nitrocellulose membrane, probed with anti-LXRα antibody (Perseus Proteomics Inc., Tokyo, Japan), and visualized by enhanced chemiluminescence. For exogenous FLAG-tagged LXR proteins, whole-cell lysates from transfected HEK293 cells were subjected to Western blotting with anti-FLAG antibody (Sigma-Aldrich), visualized by an alkaline phosphatase conjugate substrate system.

Plasmids. Fragments of the original isoform LXRα1 (GenBank accession no. NM_005693) (Willy et al., 1995), the previously reported isoform LXRα3 (GenBank accession no. NM_001130101) (Chen et al., 2005), and newly identified isoforms (LXRα4 and LXRα5) (Fig. 1) were inserted into pFLAG-CMV2 (Sigma-Aldrich) to make pFLAG-CMV2-LXRα1, pFLAG-CMV2-LXRα3, pFLAG-CMV2-LXRα4, and pFLAG-CMV2-LXRα5, respectively. The VP16 fragment from pCMX-VP16 was inserted into pFLAG-CMV2-LXRα plasmids to make pFLAG-CMV2-VP16-LXRα isoforms (Kaneko et al., 2003). The LBDs from each LXRα isoform were inserted into pCMX-GAL4 vectors to make pCMX-GAL4-LXRα isoforms. The expression vectors pCMX-β-catenin-MT, pCMX-GAL4, pCMX-GAL4-RXRα, pCMX-VP16-RXRα, pCMX-GAL4-SRC1, pCMX-GAL4-DRIP205, pCMX-GAL4-SMRT, pCMX-GAL4-N-CoR, the luciferase reporters (rCyp7a-DR4)x3-tk-LUC, TOP-GLOW, and MH100(UAS)x4-tk-LUC reporters were used as reported previously (Kaneko et al., 2003; Inaba et al., 2007; Uno et al., 2009).

Transfection Assay. Transfections in HEK293 cells were performed by the calcium phosphate coprecipitation method (Kaneko et al., 2003; Uno et al., 2009). Eight hours after transfection, compounds were added. Cells were harvested after 16 to 18 h and assayed for luciferase and β-galactosidase activities using a luminometer and a microplate reader (Molecular Devices Sunnyvale, CA). For most experiments, transfection experiments used 50 ng of reporter plasmid, 10 ng of pCMX-β-galactosidase, and 15 ng of each expression plasmid in each well of a 96-well plate. Luciferase data were normalized to the internal β-galactosidase control. SW480 cells were transfected with 2.5 μg of expression plasmid by FuGene HD (Roche Applied Science, Indianapolis, IN).

Electrophoretic Mobility Shift Assays. Electrophoretic mobility shift assays (EMSAs) were performed as reported previously (Yoshikawa et al., 2001; Chen et al., 2005). In brief, receptor proteins were in vitro-translated with a TnT Quick-Coupled Transcription/Translation System (Promega Corporation). Double-stranded oligonucleotides for LXREs were 5′-CAG TGA CCG CCA GTA ACC CCA GC-3′ (LXREa) and 5′-GGA CGC CCG CTA GTA ACC CCG GC-3′ (LXREb) from the mouse SREBP-1c promoter (Yoshikawa et al., 2001), 5′-GCT TTG GTC ACT CAA GTT CAA GTT A-3′ from the rat CYP7A promoter (Lu et al., 2000), and 5′- GAT CAC GAT GAC CGG TAG TAA CCC CGC C-3′ from the rat fatty acid synthase (Chen et al., 2005). Binding reactions were performed in a buffer containing 10 mM Tris-HCl, pH 7.6, 50 mM KCl, 0.05 mM EDTA, 2.5 mM $MgCl_2$, 8.5% glycerol, 1 mM dithiothreitol, 0.5 μg/ml poly(dI-dC), 0.1% Triton X-100, and nonfat milk (Yoshikawa et al., 2001). Unlabeled probes and anti-LXRα antibody (Perseus Proteomics Inc.) were used for competition experiments and supershift experiments, respectively. Samples were separated on 5% polyacrylamide gels, visualized with autoradiography.

Molecular Modeling. The structure of the LXRα4-LBD was manipulated using Sybyl 7.3 (Tripos, St. Louis, MO). We also used Swiss-Prot ExPASy proteomics tools for homology modeling of LXRα4-LBD and alignment of LXRα isoforms. Energy minimization of the constructed models was performed on the Tripos force field. The atomic coordinates of the crystal structures of human LXRβ-LBD complexes were retrieved from Protein Data Bank (code 1P8D) (Williams et al., 2003).

Results

Identification of Novel LXRα-LBD Variants. While examining, by PCR, the expression of the LXRα-LBD isoform reported in GenBank accession number NM_001130101 as LXRα3 by Chen et al. (2005) on a human tissue cDNA panel, we identified two novel transcripts that we will refer to as LXRα4 and LXRα5. Whereas the LXRα3 mRNA is generated by the removal of exon 6 through alternative splicing (Chen et al., 2005), the LXRα4 mRNA includes 192 nucleotides from an intron between exon 6 and exon 7 of LXRα1 (GenBank accession number NM_005693) (Willy et al., 1995) (Fig. 1, A and B). LXRα1, LXRα3, and LXRα4 proteins have 447, 387, and 511 amino acids, respectively (Fig. 1C). The LXRα5 mRNA is transcribed by alternative splicing that generates an additional exon between exon 7 and exon 8. Because a stop codon exists in this exon, LXRα5 protein truncates the C-terminal helices 7 to 12 and has 356 amino acids.

We examined mRNA expression of LXRα isoforms by real-time quantitative reverse transcription-PCR with specific primers for each isoform (Table 1). In normal human tissues, LXRα1 was highly expressed in liver, spleen, testis, pancreas, and thymus (Fig. 2A). LXRα3, LXRα4, and LXRα5 were expressed weakly in the liver, spleen, ovary, small intestine, and colon. We next examined the expression of LXRα isoforms in human hepatocyte-derived HepG2, intestinal mucosa-derived HCT116, SW480, Caco-2, myeloid-derived U937, HL60, THP-1, kidney epithelium-derived HEK293, mammary epithelium-derived MCF-7, osteoblast-derived MG63, neuron-derived NT2/D1, SK-N-SH, and keratinocyte-derived HaCaT cells. LXRα1 was the predominant isoform in all examined cells (Fig. 2B). LXRα3 was expressed in all cells except MG63 and SK-N-SH cells. It is noteworthy that LXRα4 was more abundant than LXRα3 in Caco-2 cells. LXRα5 was detected only weakly in the cell lines.

We compared the mouse LXRα gene (GenBank accession number NC_000068.6) with the human LXRα gene (GenBank accession number NC_000011.9) and designed specific primers for mouse LXRα3 and LXRα4 (Table 2). We could not find a fragment corresponding to the additional exon for human LXRα5 in the mouse LXRα gene. LXRα3 and LXRα4 were expressed weakly in the liver, kidney, intestine, spleen, heart, and lung of mice (Fig. 2C). Expression of these isoforms was at background levels in LXRα/LXRβ-double-knockout mice. It is noteworthy that LXRα4 was more abundant than LXRα3 in the mice tissues.

To examine LXRα isoform proteins, we transfected HaCaT cells with control or three different siRNAs against LXRα and determined protein accumulation of LXRα isoforms. Transfection of siLXRα-1, siLXRα-2, and, to a lesser extent, siLXRα/β decreased LXRα1 protein levels (Fig. 3A). We observed weak expression of LXRα3 and LXRα4 proteins. LXRα3 protein decreased in cells treated with siLXRα-1 but not siLXRα-2 (Fig. 3A). Although siLXRα-1 targets a mixture of sequences in exon 5, exon 6, and exon 8, siLXRα-2 is against sequences in exon 6, a region lost in LXRα3 (Fig. 1C). Treatment with siLXRα-2 and siLXRα/β reduced LXRα4 protein levels (Fig. 3). We could not detect LXRα5 protein in HaCaT cells. We also transfected HepG2 cells with siRNAs against LXRα. Similar to experiments in HaCaT cells, LXRα1 and LXRα4 protein levels decreased in HepG2 cells treated with siLXRα-1, siLXRα-2, and siLXRα/β (Fig. 3B).

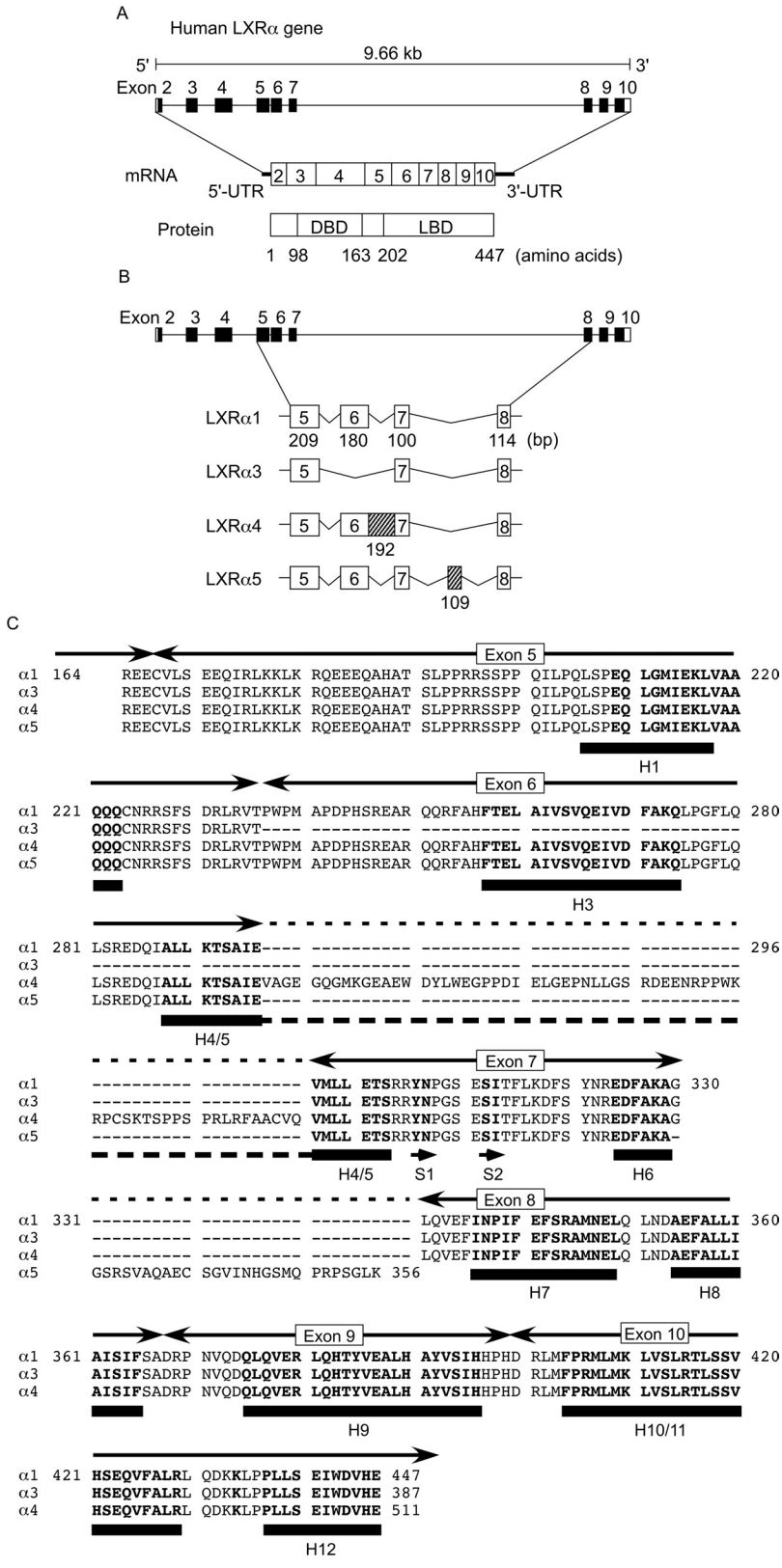

Fig. 1. LXRα-LBD isoforms. A, human LXRα gene (GenBank accession number NC_000011), LXRα1 mRNA (GenBank accession number NM_005693), and LXRα1 protein (GenBank accession number NP_005684). B, alternative splicing that generates LXRα-LBD isoforms. C, sequence alignment of LXRα-LBD isoforms. Exons that encode the corresponding amino acids are shown, and the exon numbers are as reported by Chen et al. (2005). Bars and arrows indicate helices (H) and β-sheets (S), respectively.

Treatment with siLXRα-1 and siLXRα/β also reduced LXRα3 protein levels in HepG2 cells. These findings indicate that LXRα3 and LXRα4 proteins are present in cells, although at lower levels compared with LXRα1.

The promoter of the human LXRα gene contains LXREs, and its expression is induced by LXR ligand treatment in macrophages, constituting a mechanism of positive autoregulation (Laffitte et al., 2001; Li et al., 2002). We examined the effect of a synthetic LXR ligand, T0901317, on the mRNA expression of LXRα isoforms. T0901317 increased the expression of LXRα1 in HepG2, SW480, and THP-1 cells but not in MCF-7 cells (Fig. 4). The expression of LXRα4 and LXRα5

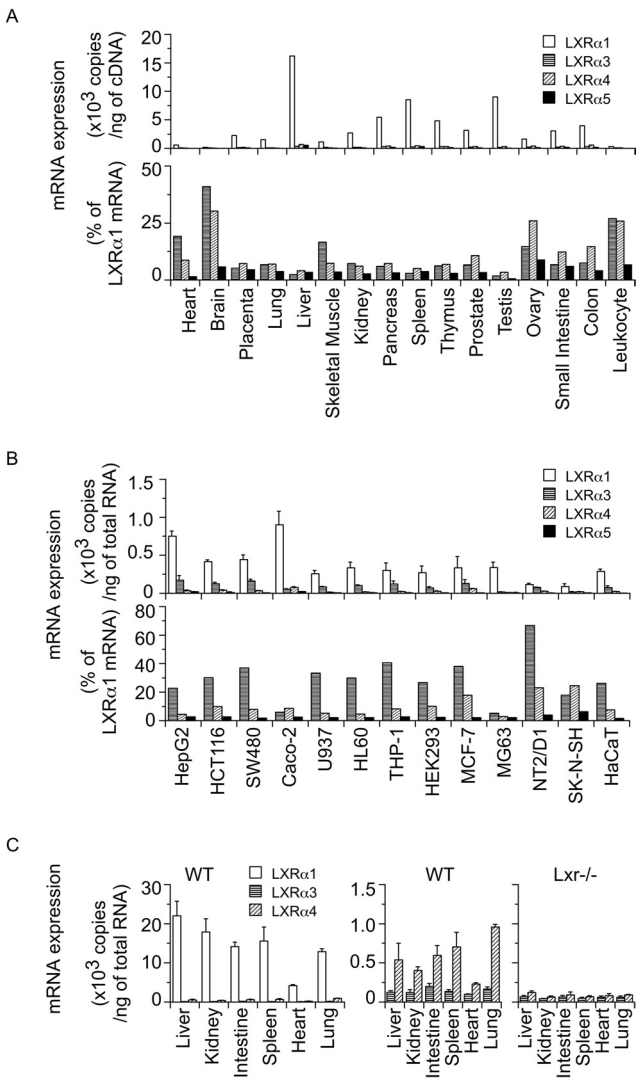

Fig. 2. Differential expression of human and mouse LXRα isoforms. A, real-time quantitative reverse transcription-PCR analysis of LXRα isoform expression in a human tissue cDNA panel. Repeated experiments showed similar results. B and C, real-time quantitative reverse transcription-PCR analysis of LXRα isoform expression in several human cell lines (B) and in several mouse tissues (C). C, LXRα3 and LXRα4 are expressed more weakly than LXRα1 (left). LXRα3 and LXRα4 expression is compared in wild-type mice (WT; middle) and Lxrα(−/−)/Lxrβ(−/−) mice (Lxr(−/−); right). The values represent means ± S.D. of triplicate assays.

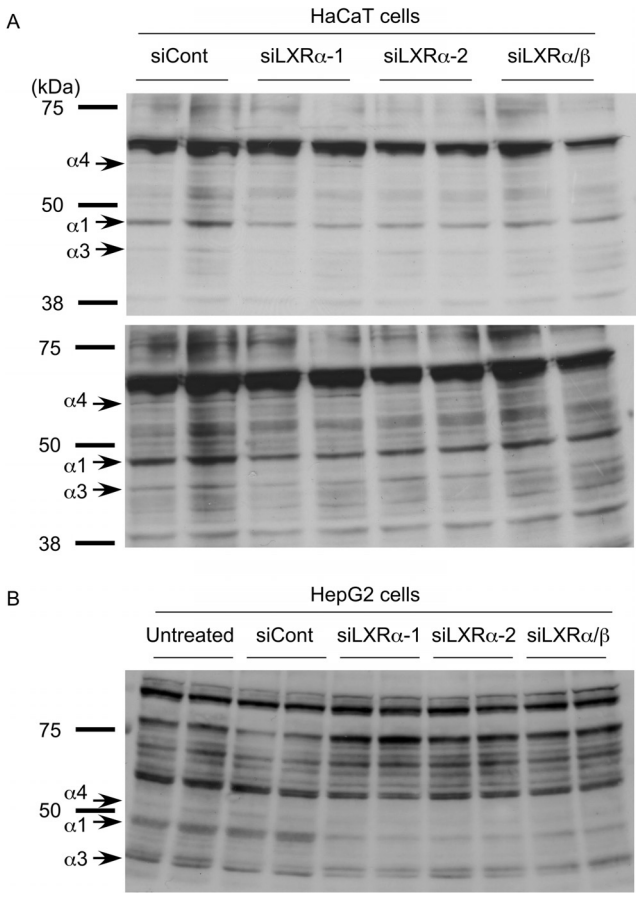

Fig. 3. Western blotting analysis of LXRα isoforms. A, expression of LXRα1, LXRα3, and LXRα4 proteins is observed in HaCaT cells. Long and short exposures are shown in top and bottom panels, respectively. B, HepG2 cells also express LXRα1, LXRα3, and LXRα4 proteins. Cells were transfected with control siRNA, (siCont), siLXRα-1, siLXRα-2, or siLXRα/β for 48 h. Nuclear proteins (30 μg) were immunoblotted with anti-LXRα antibody.

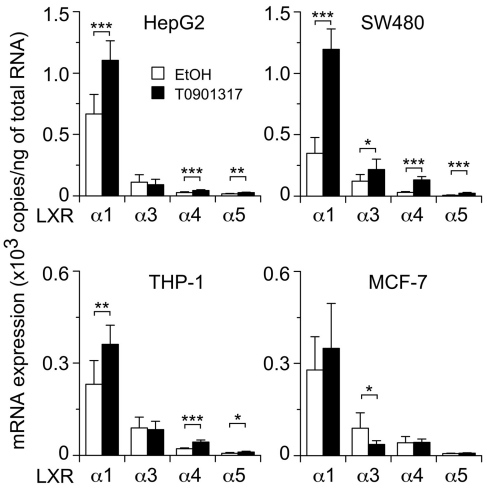

Fig. 4. Effects of an LXR ligand on mRNA expression of LXRα isoforms. Cells were treated with ethanol (EtOH) or 1 μM T0901317 for 24 h. *, $p < 0.05$; **, $p < 0.01$; ***, $p < 0.001$ compared with ethanol control. The values represent the means ± S.D. of triplicate assays.

was also induced by T0901317 in HepG2, SW480, and THP-1 cells. T0901317 increased the expression of LXRα3 in SW480 cells but had no effect in HepG2 and THP-1 cells. It is noteworthy that LXRα3 expression was decreased by T0901317 in MCF-7 cells. Thus, the expression of LXRα isoforms is regulated in a cell type-dependent manner.

Transactivation and Cofactor Interaction of LXRα Isoforms. To examine the transactivation activity of LXRα isoforms, we transiently transfected HEK293 cells with an LXR isoform expression vector and a luciferase reporter containing LXRE (Peet et al., 1998). We observed exogenous LXRα isoform proteins in HEK293 cells with immunoblotting (Fig. 5A). T0901317 effectively induced LXRα1 transactivation but had no effect on LXRα3, as reported previously (Chen et al., 2005) (Fig. 5B). T0901317 at 10 nM induced maximal LXRα1 transactivation; at 30 and 100 nM, it did not cause further induction. T0901317 activated LXRα4 less effectively than LXRα1, and LXRα5 showed no transcriptional activity. We transfected cells with a VP16-LXRα chimeric receptor together with the LXR-responsive reporter. As a result of ligand-independent activity, the luciferase activity

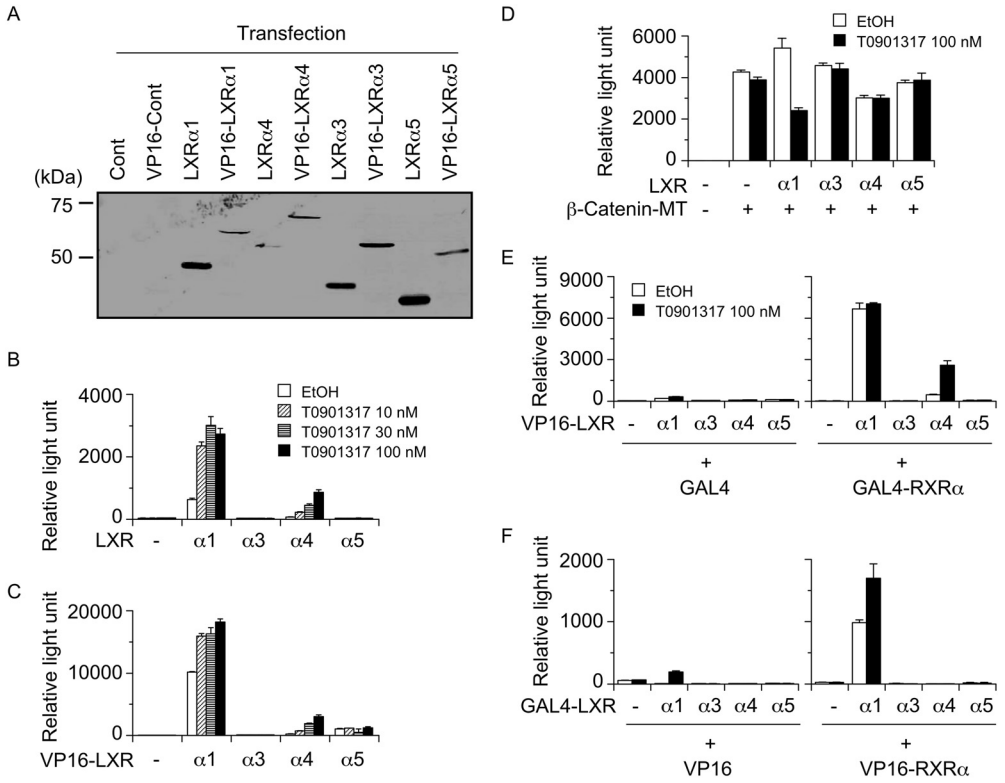

Fig. 5. Transactivation, transrepression, and RXR heterodimerization of LXRα isoforms. A, immunoblot analysis of LXRα isoforms expressed in HEK293 cells. Cells were transfected with pFLAG-CMV2 control (Cont), pFLAG-CMV2-VP16 (VP16-Cont), pFLAG-CMV-LXRα isoform, or pFLAG-CMV2-VP16-LXRα isoform. LXRα proteins were detected with anti-FLAG antibody. Each lane was loaded with 20 μg of proteins. B, transactivation of LXRα isoforms on an LXRE reporter by T0901317. HEK293 cells were transfected with pFLAG-CMV2 control (−), pFLAG-CMV2-LXRα1 (α1), pFLAG-CMV2-LXRα3 (α3), pFLAG-CMV2-LXRα4 (α4), or pFLAG-CMV2-LXRα5 (α5) and (rCyp7a-DR4)x3-tk-LUC and were treated with ethanol (EtOH) or 10, 30, or 100 nM T0901317. C, effects of constitutively active LXRα isoforms on LXRE. HEK293 cells were transfected with pFLAG-CMV2-VP16 control (−), pFLAG-CMV2-VP16-LXRα1 (α1), pFLAG-CMV2-VP16-LXRα3 (α3), pFLAG-CMV2-VP16-LXRα4 (α4), or pFLAG-CMV2-VP16-LXRα5 (α5), and treated as in B. D, repressive activity of LXRα isoforms on β-catenin transactivation. HEK293 cells were transfected with pFLAG-CMV2 control (−), pFLAG-CMV2-LXRα1 (α1), pFLAG-CMV2-LXRα3 (α3), pFLAG-CMV2-LXRα4 (α4), or pFLAG-CMV2-LXRα5 (α5), in combination with pCMX control (−) or pCMX-β-catenin-MT (+), and TOP-GLOW, and treated with ethanol (EtOH) or 100 nM T0901317. E, interaction of VP16-LXRα isoforms with GAL4 chimera of RXRα-LBD. Cells were transfected with pCMX-GAL4 control or pCMX-GAL4-RXRα in combination with pFLAG-CMV2-VP16 control (−), pFLAG-CMV2-VP16-LXRα1 (α1), pFLAG-CMV2-VP16-LXRα3 (α3), pFLAG-CMV2-VP16-LXRα4 (α4), or pFLAG-CMV2-VP16-LXRα5 (α5), and MH100(UAS)x4-tk-LUC and were treated with ethanol control (EtOH) or 100 nM T0901317. F, interaction of GAL4 chimera of LXRα-LBDs with VP16-RXRα. Cells were transfected with pCMX-GAL4 control (−), pCMX-GAL4-LXRα1 (α1), pCMX-GAL4-LXRα3 (α3), pCMX-GAL4-LXRα4 (α4), or pCMX-GAL4-LXRα5 (α5) in combination with pCMX-VP16 control or pCMX-VP16-RXRα, and MH100(UAS)x4-tk-LUC, and were treated as in E. The values represent the means ± S.D. of triplicate assays.

of VP16 chimeric receptors assesses the interaction of the receptor and the binding element (Adachi et al., 2004). VP16-LXRα1 induced luciferase activity in the absence of ligand (Fig. 5C), suggesting that VP16-LXRα1 binds to an LXRE in a ligand-independent manner. Ligand addition further increased transactivation but only slightly. VP16-LXRα3 was not effective in either the presence or the absence of ligand. These findings suggest that VP16-LXRα3 does not interact with an LXRE in cells. VP16-LXRα4 induced luciferase activity in a ligand-dependent manner, and VP16-LXRα5 induced weak ligand-independent luciferase activity. We examined the subcellular localization of LXRα isoforms using green fluorescence protein-fused proteins and found that all isoforms were localized in the nucleus (data not shown). In addition to transactivation, LXRα exhibits ligand-dependent transrepression of several transcription factors, including β-catenin (Uno et al., 2009). T0901317 treatment inhibited β-catenin transactivation of T cell factor-mediated transcription in the presence of LXRα1, as reported previously (Uno et al., 2009). Ligand-dependent inhibition was not observed with cotransfection of LXRα3, LXRα4, or LXRα5. Thus, LXRα3, LXRα4, and LXRα5 are nonfunctional LXRα isoforms (Fig. 5D).

To examine the RXR heterodimerization of LXRα isoforms, we performed mammalian two-hybrid experiments using VP16-LXRα, GAL4-RXRα, and a GAL4-responsive luciferase reporter. The full-length fragments of LXRα isoforms were fused to the VP16 transactivation domain, and the RXRα-LBD was fused to GAL4 DNA-binding domain (DBD). VP16-LXRα1 effectively interacted with GAL4-RXRα in a ligand-independent manner (Fig. 5E). T0901317 treatment did not cause further increase, suggesting maximal interaction of GAL4-RXRα and VP16-LXRα1 in the absence of ligand. VP16-LXRα4 made a weak interaction with GAL4-RXRα that was enhanced by T0901317 treatment. VP16-LXRα3 and VP16-LXRα5 did not interact with GAL4-RXRα in the presence or absence of ligand. We next examined the interaction of GAL4-LXRα and VP16-RXRα. The LBDs of LXRα isoforms were fused to GAL4-DBD, and the full-length fragment of RXRα was fused to the VP16 domain. First, we examined the transactivation activity of GAL4-LXRα isoforms with cotransfection of a control VP16 vector that does

not interact with a GAL4 chimeric receptor. Among the GAL4-LXRα isoforms, only GAL4-LXRα1 was activated by T0901317 (Fig. 5F). Next, we examined effect of cotransfection of GAL4-LXRα and VP16-RXRα. GAL4-LXRα1 plus VP16-RXRα activated the luciferase reporter, indicating a ligand-independent association of these receptors. Ligand addition further enhanced the interaction. Although full-length fragments of receptors were fused to VP16 proteins, GAL4 chimeric receptors contain only LBDs of receptors. These structures may cause the difference in interaction between GAL4-RXRα/VP16-LXRα1 and GAL4-LXRα1/VP16-RXRα. Interactions were not observed between VP16-RXRα and GAL4-LXRα3, GAL-LXRα4, or GAL-LXRα5 (Fig. 5F). Comparison of the VP16-RXRα/GAL4-LXRα4 interaction with the GAL4-RXRα/VP16-LXRα4 interaction suggests that unlike LXRα1-LBD, LXRα4-LBD cannot stably heterodimerize with RXR.

We examined direct binding of LXRα isoforms to LXREs by EMSAs. As reported previously (Yoshikawa et al., 2001), LXRα1-RXR heterodimer bound to a LXRE from the SREBP-1c promoter (Fig. 6A). Incubation with anti-LXRα antibody induced a supershift of the LXRα1-RXR DNA complex, and addition of unlabeled probes competed the binding of LXRα1-RXR to labeled probes, confirming the specific binding of LXRα1-RXR to the LXRE. Complex formation of LXRα1-RXR-LXRE did not require ligand addition (Fig. 6B), consistent with a ligand-independent effect of VP16-LXRα1 on an LXRE reporter in cells (Fig. 5B). In contrast, DNA complex was not observed for LXRα3, LXRα4 and LXRα5 in combination with RXR, and T0901317 treatment was not effective (Fig. 6B).

We examined the effect of other LXR ligands on transactivation of LXRα isoforms. A synthetic agonist, GW3965, and natural ligands 24(*S*),25-epoxycholsterol and 22(*R*)-hydroxycholesterol activated LXRα4 but more weakly than their activation of LXRα1 (Fig. 7A). 22(*S*)-Hydroxycholesterol, arachidonic acid, and linolenic acid are LXR antagonists (Ou et al., 2001; Spencer et al., 2001). These LXR antagonists did not activate LXRα isoforms (Fig. 7A). 22(*S*)-Hydroxycholesterol and arachidonic acid inhibited transactivation of LXRα1 and LXRα4 induced by GW3965 and 24(*S*),25-epoxycholesterol (Fig. 7B).

Upon ligand binding, nuclear receptors undergo conformational changes in the cofactor binding site and the activation function 2 (AF2) helix that result in the dissociation of corepressors [such as silencing mediator of retinoic acid and thyroid hormone receptor (SMRT) and nuclear receptor corepressor (N-CoR)] and recruitment of coactivators [such as steroid receptor coactivator 1 (SRC-1) and vitamin D receptor-interacting protein 205 (DRIP205)] (Rosenfeld et al., 2006). We fused the receptor-interacting domains of transcriptional cofactors to the GAL4-DBD and examined the interaction of LXRα isoforms with cofactors in a mammalian two-hybrid assay. VP16-LXRα1 associated with GAL4-SRC-1 and GAL4-DRIP205, and addition of ligand or cotransfection of RXRα enhanced these interactions (Fig. 8, A and B). VP16-LXRα4 weakly interacted with GAL4-SRC-1 and GAL4-DRIP205 only when cells were cotransfected with RXRα. T0901317 had a small effect on these interactions. This coactivator recruitment may be related to weak transactivation of LXRα4 (Fig. 5B). The LXRα3 and LXRα5 did not interact with the coactivators. VP16-LXRα1 interacted with GAL4-N-

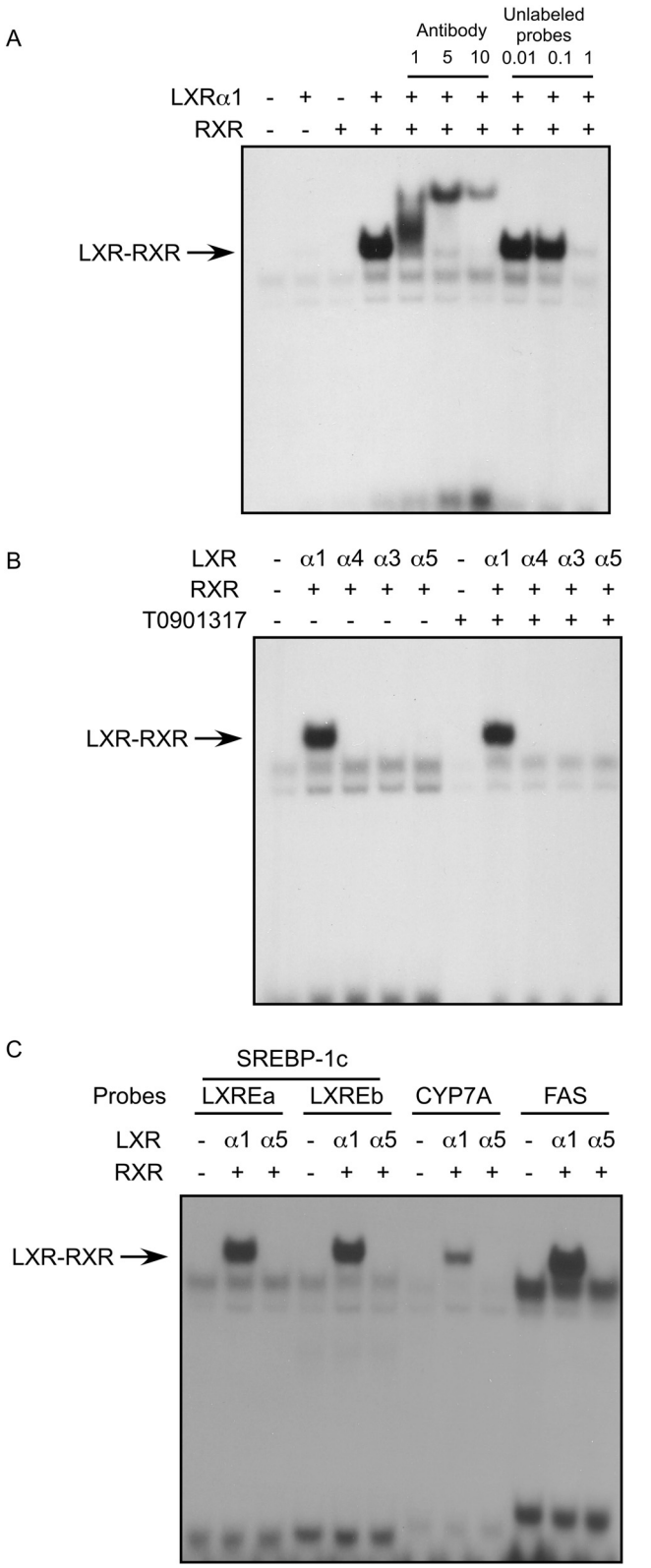

Fig. 6. LXRα1, but not LXRα3, LXRα4 or LXRα5, binds to LXREs. A, LXREα from the mouse SREBP-1c was labeled and incubated with LXRα1 and/or RXRα proteins. Preincubation with anti-LXRα antibody (1, 5, or 10 μg) and unlabeled LXREa probes (0.01, 0.1, or 1 μM) was performed for supershift and competition, respectively. B, LXRα1, but not LXRα3, LXRα4, or LXRα5, in combination with RXRα, binds to LXREa from SREBP-1c. Treatment with 1 μM T0901317 does not affect a complex formation. C, EMSAs using LXREs from the mouse SREBP-1c promoter (LXREa and LXREb), the rat CYP7A promoter and the rat fatty acid synthase (FAS) promoter.

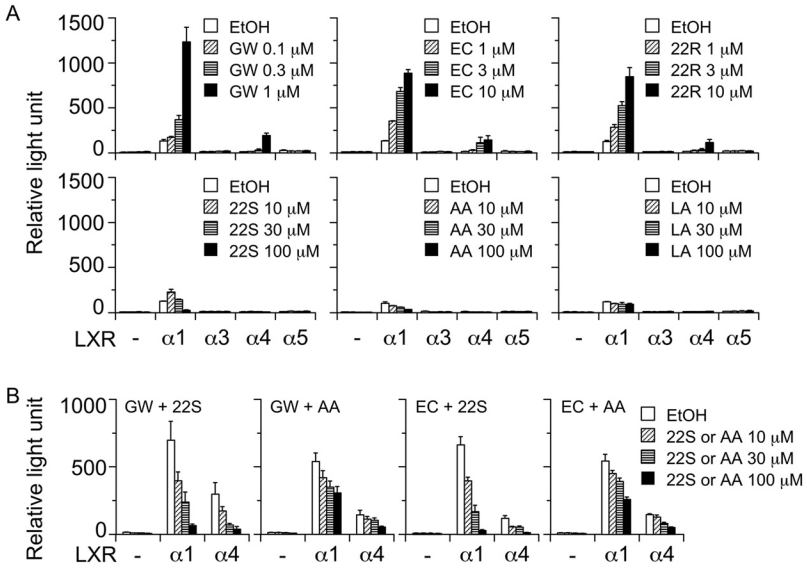

Fig. 7. Effects of GW3965, oxysterols, and fatty acids on transactivation of LXRα isoforms. A, LXR agonists, GW3965, 24(*S*),25-epoxycholesterol, and 22(*R*)-hydroxycholesterol induce activation of LXRα1 and LXRα4 but not LXRα3 or LXRα5. LXRα antagonists 22(*S*)-hydroxycholesterol, arachidonic acid, and linolenic acid are not effective on transactivation of LXRα isoforms. HEK293 cells were transfected as in Fig. 5B and treated with ethanol (EtOH), GW3965 (GW), 24(*S*),25-epoxycholesterol (EC), 22(*R*)-hydroxycholesterol (22R), 22(*S*)-hydroxycholesterol (22S), arachidonic acid (AA), or linolenic acid (LA). B, LXRα antagonists suppress transactivation of LXRα1 and LXRα4 induced by GW3965 and 24(*S*),25-epoxycholesterol. HEK293 cells were transfected as in Fig. 5B and treated with 1 μM GW3965 (GW) or 10 μM 24(*S*),25-epoxycholesterol (EC) in combination with ethanol (EtOH), 22(*S*)-hydroxycholesterol (22S) or arachidonic acid (AA). The values represent means ± S.D. of triplicate assays.

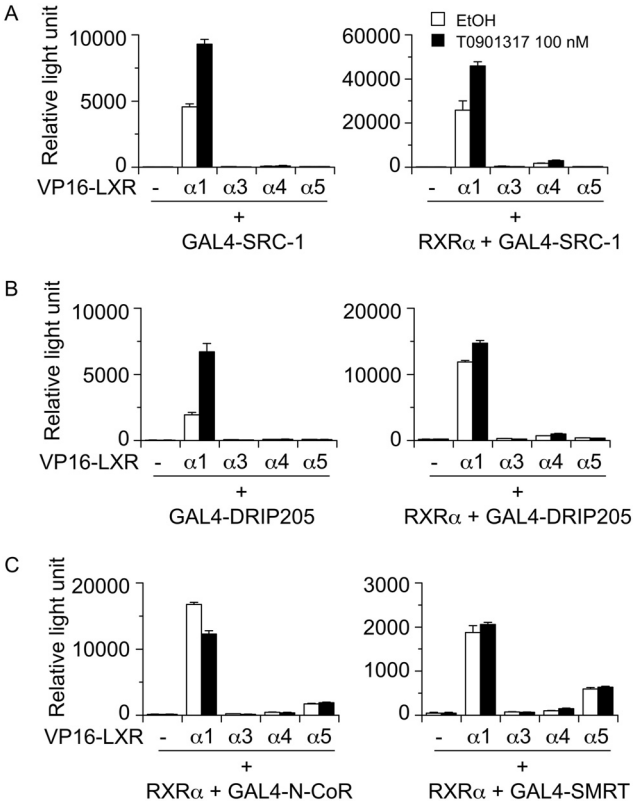

Fig. 8. Interaction of LXRα isoforms with cofactors. Interaction of LXRα isoforms with coactivators SRC-1 (A) and DRIP205 (B). Cells were transfected with pFLAG-CMV2-VP16 control (−), pFLAG-CMV2-VP16-LXRα1 (α1), pFLAG-CMV2-VP16-LXRα3 (α3), pFLAG-CMV2-VP16-LXRα4 (α4), or pFLAG-CMV2-VP16-LXRα5 (α5) in combination with pCMX-GAL4-SRC-1 (A) or pCMX-GAL4-DRIP205 and MH100(UAS)x4-tk-LUC and were treated with ethanol control (EtOH) or 100 nM T0901317. Cells were cotransfected without (left) or with pCMX-RXRα (right). C, interaction of LXRα isoforms with corepressors. Cells were transfected with pFLAG-CMV2-VP16 control (−), pFLAG-CMV2-VP16-LXRα1 (α1), pFLAG-CMV2-VP16-LXRα3 (α3), pFLAG-CMV2-VP16-LXRα4 (α4), or pFLAG-CMV2-VP16-LXRα5 (α5), in combination with pCMX-RXRα, pCMX-GAL4-N-CoR, or pCMX-GAL4-SMRT, and MH100(UAS)x4-tk-LUC, and were treated as in A. The values represent the means ± S.D. of triplicate assays.

CoR, VP16-LXRα5 interacting weakly (Fig. 8C). T0901317 caused a modest dissociation of N-CoR from VP16-LXRα1, but not from VP16-LXRα5. VP16-LXRα1 and VP16-LXRα5 also interacted with GAL4-SMRT, but ligand addition did not affect these interactions (Fig. 8C). VP16-LXRα3 and VP16-LXRα4 did not associate with these corepressors. These experiments illustrate differential interactions of LXRα isoforms with cofactors.

We next examined the dominant-negative effect of LXRα3, LXRα4, and LXRα5 on LXRα1 transactivation. When expressed together with LXRα1 in transfection assays, LXRα3 and LXRα4 did not act as dominant-negative inhibitors, and LXRα5 inhibited LXRα1 transactivation when expressed in excess (Fig. 9A). In EMSAs, we did not detect a complex of LXRα5, RXR, and LXREs from SREBP-1c, CYP7A, or fatty acid synthase (Fig. 6C). Expression of LXRα5 also suppressed ligand-dependent induction of LXR target genes, SREBP-1c, and ABCA1 in SW480 cells, whereas LXRα1 enhanced expression of these genes (Fig. 9B). Combination of LXRα5 cotransfection and LXRα antagonist treatment produced additive effects on the inhibition of LXRα1 transactivation induced by LXR agonists (Fig. 9C).

Structural Model of LXRα4. Of LXRα3, LXRα4, and LXRα5, only LXRα4 displays transactivation potential (Fig. 5). LXRα4 has an identical amino acid sequence with LXRα1 with the exception of a 64-amino acid residue insertion between Glu 296 and Val 297 at helix 4/5 of LXRα1 (Fig. 1). To make homology models of the LXRα4-LBD and its heterodimer with RXR-LBD, we first constructed a monomeric model of LXRα4-LBD (amino acids 206–511), called model M1, by using an automatic modeling system (Swiss Model version 8.05) on the Swiss-Prot ExPASy workspace and the coordinates of previously solved LXRβ-LBD/24(*S*),25-epoxycholesterol structure (Protein Data Bank code 1P8D; 58.88% sequence identity with the LXRα4-LBD) (Williams et al., 2003). We docked the LXR ligand T0901317 into M1 by extracting the crystal structure of the LXRα-LBD/RXRβ-LBD/T0901317 complex (Protein Data Bank code 1UHL) (Svensson et al., 2003) and optimized the liganded complex on the Tripos force field (1000 iteration steps) using Sybyl 7.3 (Tripos) to yield model M2 (Fig. 10A). The stereochemistry of

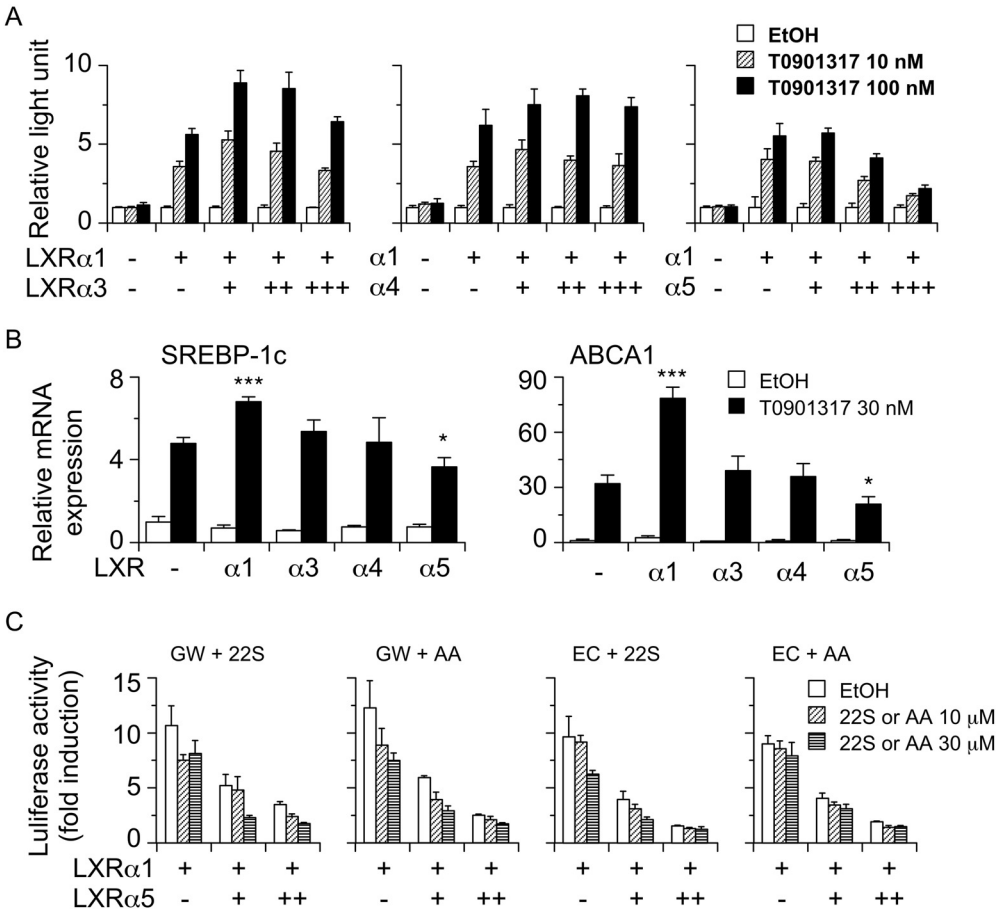

Fig. 9. Effects of overexpression of LXRα isoforms on LXRα1 transactivation and expression of LXR target genes. A, transactivation activity of LXRα1 is not inhibited by overexpression of LXRα3 or LXRα4 but is inhibited by LXRα5. HEK293 cells were transfected with 0.1 ng of pFLAG-CMV2 control (−) or pFLAG-CMV2-LXRα1 (+), in combination with 0 (−), 15 (+), 30 (++), or 60 ng (+++) of pFLAG-CMV2-LXRα3 (α3), pFLAG-CMV2-LXRα4 (α4), or pFLAG-CMV2-LXRα5 (α5), and (rCyp7a-DR4)x3-tk-LUC, and were treated with ethanol (EtOH) or 10, 30, or 100 nM T0901317. The total amounts of plasmids were adjusted by addition of pFLAG-CMV2 control vector. B, SW480 cells were transfected with 2.5 μg of control plasmid (−), pFLAG-CMV2-LXRα1 (α1), pFLAG-CMV2-LXRα3 (α3), pFLAG-CMV2-LXRα4 (α4), or pFLAG-CMV2-LXRα5 (α5) and were treated with ethanol (EtOH) or 30 nM T0901317 for 24 h. Endogenous SREBP-1c and ABCA1 mRNA levels were determined by quantitative real-time PCR analysis. Effects of T0901317 on induction of these genes were significant in all transfection experiments. *, $p < 0.05$; ***, $p < 0.001$ compared with control plasmid. C, combination of LXRα5 cotransfection and LXRα antagonist treatment exhibits additive effects on inhibition of agonist-induced LXRα1 activation. HEK293 cells were transfected with 0.1 ng of pFLAG-CMV2-LXRα1 (+) in combination with 0 (−), 40 (+), or 60 ng (++) of pFLAG-CMV2-LXRα5 (α5), and (rCyp7a-DR4)x3-tk-LUC, and were treated with 1 μM GW3965 (GW) or 10 μM 24(*S*),25-epoxycholesterol (EC) in combination with ethanol (EtOH), 22(*S*)-hydroxycholesterol (22S), or arachidonic acid (AA). The values represent means ± S.D. of triplicate assays.

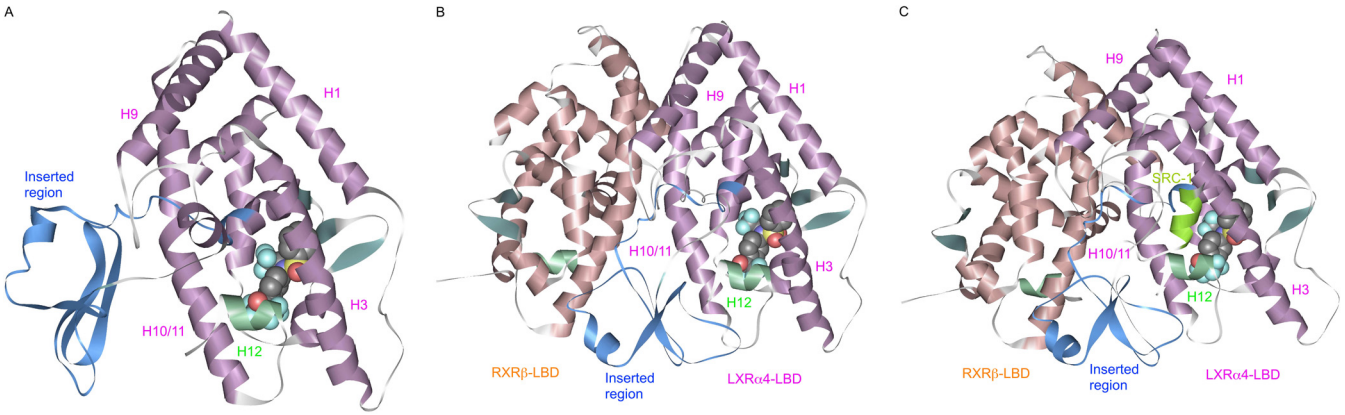

Fig. 10. Structural model of LXRα4. A, model of LXRα4-LBD docked with T0901317 (model M2) was created by automatic selection of LXRβ-LBD/24(*S*),25-epoxycholesterol complex (Protein Data Bank code 1P8D) as a template and optimization of the complex docked with T0901317, whose structure was extracted from the LXRα-LBD/RXRβ-LBD/T0901317 complex (Protein Data Bank code 1UHL). B, model of LXRα4/RXR heterodimer (model M3) was created by overlaying the liganded model, in which LXRβ in LXRβ-LBD/24(*S*),25-epoxycholesterol (Protein Data Bank code 1P8D) was replaced with LXRα4, with the LXRα-LBD/RXRβ-LBD/T0901317 (Protein Data Bank code 1UHL). C, in model M4, the SRC-1 coactivator peptide was placed at LXRα4 in the same place as LXRα1. H, helix.

M2 satisfied a Ramachandran plot analysis. In M2, the 64-amino acid insertion extrudes rearward from the side of helix 10/11 covering the dimer interface. Crystal structure analysis is needed to elucidate whether the inserted region is totally outside the canonical structure of the LBD. LXRα4 forms an RXR heterodimer and induces an LXRE reporter activation, although weakly, as shown in Fig. 5. The RXR heterodimerization interface uses helix 10/11, helix 9, loop 8 to 9, and helix 7 of the LBD (Gampe et al., 2000). The recently solved crystal structure of the peroxisome proliferator-activated receptor γ (PPARγ)/RXRγ/DNA complex (Protein Data Bank code 3DZY) shows an additional dimer interface between PPARγ-LBD (loops 1–3 and β-turn) and RXRγ-DBD (Chandra et al., 2008). The LXRα4 insertion is suggested to prevent heterodimerization at the interface with RXR. LXRα4 may interact only at the β-turn side of the LBD with the DBD of the dimer partner, as has been shown for PPARγ in the RXR heterodimer crystal structure.

We next constructed a canonical heterodimer model of LXRα4-LBD/RXRβ-LBD, using the LXRα1-LBD/RXRβ-LBD structure (Protein Data Bank code 1UHL) as a model. We overlaid LXRα4-LBD in the liganded model M1 with LXRα1-LBD in the crystal structure, replaced the LXRα1-LBD with LXRα4-LBD, and changed the dihedral angle (ψ and ϕ) at Ser 282 of LXRα4-LBD to relieve hindrance between the insertion and RXRβ. We optimized the complex of LXRα4-LBD/RXRβ-LBD accommodated with each ligand (3000 iteration steps) by fixing RXRβ and the two ligands to generate heterodimer model M3 (Fig. 10B). With this optimization, the insertion changed conformation significantly and was packed in the cavity beneath the contact of helix 10/11 from each monomer. The main chain conformations of M3 were found to be in satisfactory region by Ramachandran plot analysis. The peptide fragment of SRC-1 was extracted form the LXRβ-LBD/24(*S*),25-epoxycholesterol complex structure (Protein Data Bank code 1P8D) and was docked into M3 to create the model M4. In M4, important residues of the AF2 helix, such as charge clamp residues, Lys 273 at helix 3 and Glu 441 at helix 12, occupy the correct positions and an LXXLL-containing coactivator peptide of SRC-1 is predicted to stably interact (Fig. 10C).

Discussion

We report two novel LXRα-LBD isoforms, LXRα4 and LXRα5. LXRα4 maintains transactivation, DNA binding, and RXR heterodimerization with weaker activity than LXRα1. Structural modeling reveals that the 64-amino acid insertion at helix 4/5 disturbs RXR heterodimerization. LXRα agonist treatment increased the activity of LXRα4, suggesting that ligand binding stabilizes the conformation of the LXRα4/RXR heterodimer. Although ligand treatment recruited coactivators to LXRα4, interaction of LXRα4 with corepressors was not observed. The LXRα4 insertion may disturb corepressor interaction. LXRα5, a C-terminal truncated form, lacks helices 7 to 12, the AF2 domain, and dimerization interface. As expected, LXRα5 is deficient in transactivation and coactivator recruitment. It is noteworthy that LXRα5 is associated with corepressors. LXRα5 cotransfection inhibited LXRα1 activity in the overexpression experiment and ligand-dependent expression of endogenous LXR target genes (Fig. 9). LXRα3 lacks the residues necessary for helices 3 and 4/5. LXRα3 has an intact DBD and binds to an LXRE in combination with RXR in an in vitro EMSA (Chen et al., 2005). In contrast, we did not observe formation of a LXRα3-RXR-LXRE complex in the absence or presence of LXR ligand (Fig. 6B). This discrepancy between our study and that of Chen et al. (2005) may be due to a difference in experimental conditions. Consistent with our EMSA results, LXRα3 did not heterodimerize with RXRα or bind to LXRE in cells (Fig. 5). The conformation of LXRα3 may be unstable and be influenced by experimental conditions.

Compared with the full-length LXRα1, expression of other LXRα isoforms (LXRα3, LXRα4, and LXRα5; in mice, LXRα3 and LXRα4) was diminished in normal tissues (Fig. 2, A and C). Chen et al. (2005) reported that LXRα3 is expressed in lung higher than other tissues, whereas LXRα2 is abundant in testis. In our results, human LXRα3 was highly expressed in brain, heart, leukocyte, skeletal muscle, and ovary, whereas mouse LXRα3 was high in lung and spleen (Fig. 2, A and C). Further studies are needed to elucidate how LXRα isoform expression is physiologically regulated and whether there are age, sex, and racial differences. It is noteworthy that relative expression levels were increased in several cell lines (Fig. 2B). Although LXRα isoforms were only weakly expressed in the neuron-derived NT2/D1 and SK-N-SH cells, the relative expression of LXRα3 was 60% of LXRα1 levels in NT2/D1 cells. Chen et al. (2005) reported that LXRα3 is expressed to relatively high levels in glioma cells. Because ligand-activated LXRα1 inhibits cellular proliferation (Blaschke et al., 2004; Fukuchi et al., 2004; Uno et al., 2009), expression of the functional form of LXRα1 may be repressed in some malignant cells, such as neuron-derived tumors. LXRα3, LXRα4, and LXRα5 are hypomorphic isoforms that lack dominant-negative activity on LXRα1. It is unlikely that the expression of these isoforms disturbs LXRα1 function or contributes to the pathogenesis of human diseases, although the possibility remains that they may gain other unidentified functions. Alternatively, isoform expression may be a consequence of dysfunction of splicing and/or pre-mRNA degradation. Pre-mRNA splicing in mammalian cells is regulated by a ribonucleoprotein complex known as the spliceosome (Wahl et al., 2009). Patterns of alternative splicing vary in cell types and across development, likely because of dynamic changes in the spliceosome protein complement. Alternative splicing is linked to various human diseases, including cancer (Cooper et al., 2009). Extra- and intracellular signaling regulates pre-mRNA splicing by modulating the dynamic assembly of the spliceosome components (Shin and Manley, 2004). In addition to splicing regulation, the RNA quality control system also regulates mRNA expression to prevent the production of truncated proteins with dominant-negative or deleterious gain-of-function activities (Chang et al., 2007). The nonsense-mediated mRNA decay system degrades mRNAs carrying premature translation termination codons. The LXRα5 mRNA contains a stop codon in a novel exon between exons 6 and 7 of LXRα1 (Fig. 1). LXRα5 expression was limited in all of the examined human tissues and cell lines (Fig. 2), a finding that may be due to nonsense-mediated mRNA decay. LXRα dysfunction has been implicated in lipid metabolism disorders, autoimmune diseases, atherosclerosis, and cancers (Tontonoz and Mangelsdorf, 2003; Fukuchi et al., 2004; Bensinger et al., 2008; Vedin et al., 2009). RNA quality-control mechanisms may lead to preferential LXRα1

expression, and increased LXRα3, LXRα4, and LXRα5 expression could be biomarkers of LXRα-related diseases. T0901317 treatment differently regulated the expression of LXRα-LBD isoforms in cells (Fig. 3), suggesting that LXRα ligand activation influences the expression of alternatively spliced products in a cell type-dependent manner. Further studies are required to elucidate the role of LXRα in post-transcriptional RNA control.

We created a structural model of LXRα4 using the crystal structures of related nuclear receptors, such as LXRα1 and LXRβ. The modeling technique used in this study can be applied for analysis of variants of other nuclear receptors. Further functional studies and computer modeling in combination with X-ray crystal structure analysis should be useful in the development of molecularly targeted nuclear receptor therapies.

Acknowledgments

We thank members of the Makishima laboratory for technical assistance and helpful comments, Dr. David J. Mangelsdorf of the Howard Hughes Medical Institute and University of Texas Southwestern Medical Center at Dallas for providing Lxrα(−/−)/Lxrβ(−/−) mice, and Dr. Andrew I. Shulman for editorial assistance.

Authorship Contributions

Participated in research design: Endo-Umeda, Fujimori, Naito, Saito, Yamada, and Makishima.

Conducted experiments: Endo-Umeda, Uno, Fujimori, and Naito.

Contributed new reagents or analytic tools: Endo-Umeda, Jeong, and Miyachi.

Performed data analysis: Endo-Umeda, Naito, Saito, Yamagishi, Tokiwa, Yamada, and Makishima.

Wrote or contributed to the writing of the manuscript: Endo-Umeda, and Makishima.

References

Adachi R, Shulman AI, Yamamoto K, Shimomura I, Yamada S, Mangelsdorf DJ, and Makishima M (2004) Structural determinants for vitamin D receptor response to endocrine and xenobiotic signals. *Mol Endocrinol* **18:**43–52.

Bensinger SJ, Bradley MN, Joseph SB, Zelcer N, Janssen EM, Hausner MA, Shih R, Parks JS, Edwards PA, Jamieson BD, et al. (2008) LXR signaling couples sterol metabolism to proliferation in the acquired immune response. *Cell* **134:**97–111.

Blaschke F, Leppanen O, Takata Y, Caglayan E, Liu J, Fishbein MC, Kappert K, Nakayama KI, Collins AR, Fleck E, et al. (2004) Liver X receptor agonists suppress vascular smooth muscle cell proliferation and inhibit neointima formation in balloon-injured rat carotid arteries. *Circ Res* **95:**e110–123.

Chandra V, Huang P, Hamuro Y, Raghuram S, Wang Y, Burris TP, and Rastinejad F (2008) Structure of the intact PPAR-γ-RXR-α nuclear receptor complex on DNA. *Nature* **456:**350–356.

Chang YF, Imam JS, and Wilkinson MF (2007) The nonsense-mediated decay RNA surveillance pathway. *Annu Rev Biochem* **76:**51–74.

Chen M, Beaven S, and Tontonoz P (2005) Identification and characterization of two alternatively spliced transcript variants of human liver X receptor alpha. *J Lipid Res* **46:**2570–2579.

Cooper TA, Wan L, and Dreyfuss G (2009) RNA and disease. *Cell* **136:**777–793.

Fukuchi J, Kokontis JM, Hiipakka RA, Chuu CP, and Liao S (2004) Antiproliferative effect of liver X receptor agonists on LNCaP human prostate cancer cells. *Cancer Res* **64:**7686–7689.

Gampe RT Jr, Montana VG, Lambert MH, Miller AB, Bledsoe RK, Milburn MV, Kliewer SA, Willson TM, and Xu HE (2000) Asymmetry in the PPARγ/RXRα crystal structure reveals the molecular basis of heterodimerization among nuclear receptors. *Mol Cell* **5:**545–555.

Inaba Y, Yamamoto K, Yoshimoto N, Matsunawa M, Uno S, Yamada S, and Makishima M (2007) Vitamin D_3 derivatives with adamantane or lactone ring side chains are cell type-selective vitamin D receptor modulators. *Mol Pharmacol* **71:**1298–1311.

Ishizawa M, Matsunawa M, Adachi R, Uno S, Ikeda K, Masuno H, Shimizu M, Iwasaki K, Yamada S, and Makishima M (2008) Lithocholic acid derivatives act as selective vitamin D receptor modulators without inducing hypercalcemia. *J Lipid Res* **49:**763–772.

Joseph SB, Bradley MN, Castrillo A, Bruhn KW, Mak PA, Pei L, Hogenesch J, O'Connell RM, Cheng G, Saez E, et al. (2004) LXR-dependent gene expression is important for macrophage survival and the innate immune response. *Cell* **119:**299–309.

Kaneko E, Matsuda M, Yamada Y, Tachibana Y, Shimomura I, and Makishima M (2003) Induction of intestinal ATP-binding cassette transporters by a phytosterol-derived liver X receptor agonist. *J Biol Chem* **278:**36091–36098.

Laffitte BA, Joseph SB, Walczak R, Pei L, Wilpitz DC, Collins JL, and Tontonoz P (2001) Autoregulation of the human liver X receptor α promoter. *Mol Cell Biol* **21:**7558–7568.

Li Y, Bolten C, Bhat BG, Woodring-Dietz J, Li S, Prayaga SK, Xia C, and Lala DS (2002) Induction of human liver X receptor alpha gene expression via an autoregulatory loop mechanism. *Mol Endocrinol* **16:**506–514.

Lu TT, Makishima M, Repa JJ, Schoonjans K, Kerr TA, Auwerx J, and Mangelsdorf DJ (2000) Molecular basis for feedback regulation of bile acid synthesis by nuclear receptors. *Mol Cell* **6:**507–515.

Makishima M (2005) Nuclear receptors as targets for drug development: regulation of cholesterol and bile acid metabolism by nuclear receptors. *J Pharmacol Sci* **97:**177–183.

Noguchi-Yachide T, Aoyama A, Makishima M, Miyachi H, and Hashimoto Y (2007) Liver X receptor antagonists with a phthalimide skeleton derived from thalidomide-related glucosidase inhibitors. *Bioorg Med Chem Lett* **17:**3957–3961.

Ou J, Tu H, Shan B, Luk A, DeBose-Boyd RA, Bashmakov Y, Goldstein JL, and Brown MS (2001) Unsaturated fatty acids inhibit transcription of the sterol regulatory element-binding protein-1c (SREBP-1c) gene by antagonizing ligand-dependent activation of the LXR. *Proc Natl Acad Sci USA* **98:**6027–6032.

Peet DJ, Turley SD, Ma W, Janowski BA, Lobaccaro JM, Hammer RE, and Mangelsdorf DJ (1998) Cholesterol and bile acid metabolism are impaired in mice lacking the nuclear oxysterol receptor LXRα. *Cell* **93:**693–704.

Repa JJ and Mangelsdorf DJ (2002) The liver X receptor gene team: potential new players in atherosclerosis. *Nat Med* **8:**1243–1248.

Repa JJ, Turley SD, Lobaccaro JA, Medina J, Li L, Lustig K, Shan B, Heyman RA, Dietschy JM, and Mangelsdorf DJ (2000) Regulation of absorption and ABC1-mediated efflux of cholesterol by RXR heterodimers. *Science* **289:**1524–1529.

Rosenfeld MG, Lunyak VV, and Glass CK (2006) Sensors and signals: a coactivator/corepressor/epigenetic code for integrating signal-dependent programs of transcriptional response. *Genes Dev* **20:**1405–1428.

Schultz JR, Tu H, Luk A, Repa JJ, Medina JC, Li L, Schwendner S, Wang S, Thoolen M, Mangelsdorf DJ, et al. (2000) Role of LXRs in control of lipogenesis. *Genes Dev* **14:**2831–2838.

Shin C and Manley JL (2004) Cell signalling and the control of pre-mRNA splicing. *Nat Rev Mol Cell Biol* **5:**727–738.

Spencer TA, Li D, Russel JS, Collins JL, Bledsoe RK, Consler TG, Moore LB, Galardi CM, McKee DD, Moore JT, et al. (2001) Pharmacophore analysis of the nuclear oxysterol receptor LXRα. *J Med Chem* **44:**886–897.

Svensson S, Ostberg T, Jacobsson M, Norström C, Stefansson K, Hallén D, Johansson IC, Zachrisson K, Ogg D, and Jendeberg L (2003) Crystal structure of the heterodimeric complex of LXRα and RXRβ ligand-binding domains in a fully agonistic conformation. *EMBO J* **22:**4625–4633.

Tontonoz P and Mangelsdorf DJ (2003) Liver X receptor signaling pathways in cardiovascular disease. *Mol Endocrinol* **17:**985–993.

Uno S, Endo K, Jeong Y, Kawana K, Miyachi H, Hashimoto Y, and Makishima M (2009) Suppression of β-catenin signaling by liver X receptor ligands. *Biochem Pharmacol* **77:**186–195.

Valledor AF, Hsu LC, Ogawa S, Sawka-Verhelle D, Karin M, and Glass CK (2004) Activation of liver X receptors and retinoid X receptors prevents bacterial-induced macrophage apoptosis. *Proc Natl Acad Sci USA* **101:**17813–17818.

Vedin LL, Lewandowski SA, Parini P, Gustafsson JA, and Steffensen KR (2009) The oxysterol receptor LXR inhibits proliferation of human breast cancer cells. *Carcinogenesis* **30:**575–579.

Wahl MC, Will CL, and Lührmann R (2009) The spliceosome: design principles of a dynamic RNP machine. *Cell* **136:**701–718.

Williams S, Bledsoe RK, Collins JL, Boggs S, Lambert MH, Miller AB, Moore J, McKee DD, Moore L, Nichols J, et al. (2003) X-ray crystal structure of the liver X receptor β ligand binding domain: regulation by a histidine-tryptophan switch. *J Biol Chem* **278:**27138–27143.

Willy PJ, Umesono K, Ong ES, Evans RM, Heyman RA, and Mangelsdorf DJ (1995) LXR, a nuclear receptor that defines a distinct retinoid response pathway. *Genes Dev* **9:**1033–1045.

Yoshikawa T, Shimano H, Amemiya-Kudo M, Yahagi N, Hasty AH, Matsuzaka T, Okazaki H, Tamura Y, Iizuka Y, Ohashi K, et al. (2001) Identification of liver X receptor-retinoid X receptor as an activator of the sterol regulatory element-binding protein 1c gene promoter. *Mol Cell Biol* **21:**2991–3000.

Address correspondence to: Makoto Makishima, Division of Biochemistry, Department of Biomedical Sciences, 30-1 Oyaguchi-kamicho, Itabashi-ku, Tokyo 173-8610, Japan. E-mail address: makishima.makoto@nihon-u.ac.jp